

DYNAMICS OF FUNDAMENTAL OPTICAL TRANSITIONS IN GROUP III-NITRIDES

H. X. Jiang and J. Y. Lin

Department of Physics, Kansas State University, Manhattan, KS 66506-2601

ABSTRACT

With the recent rapid development of GaN based optoelectronic devices, a full understanding of the dynamics of fundamental optical transitions in GaN epilayers and quantum wells becomes increasingly important. In this paper, the dynamics of fundamental optical transitions, probed by picosecond time-resolved photoluminescence (PL), in GaN and InGaN epilayers, $\text{In}_x\text{Ga}_{1-x}\text{N}/\text{GaN}$ and $\text{GaN}/\text{Al}_x\text{Ga}_{1-x}\text{N}$ multiple quantum wells (MQWs) are reviewed. For GaN epilayers, optical transitions in n- and p-type (Mg doped) and semi-insulating GaN epilayers are discussed. Time-resolved PL results on the fundamental optical transitions in these materials, including the impurity-bound excitons and free excitons transitions, are summarized. For MQWs, recombination dynamics of optical transitions in both $\text{In}_x\text{Ga}_{1-x}\text{N}/\text{GaN}$ and $\text{GaN}/\text{Al}_x\text{Ga}_{1-x}\text{N}$ MQWs grown by different methods (MOCVD vs. MBE) are compared with each other as well as with GaN and InGaN epilayers to extrapolate the mechanisms and quantum efficiencies of the optical emissions in these structures. The implications of these results on device applications, in particular on the blue LEDs and laser diodes as well on the lasing mechanisms in GaN blue lasers, are also discussed.

Keywords: GaN, wide bandgap, carrier dynamics, optical transition, excitons

1. INTRODUCTION

GaN based devices offer a great potential for applications such as UV-blue lasers, solar-blind UV detectors, and high-power electronics. Researchers in this field have made extremely rapid progress toward materials growth as well as device fabrication.¹ The commercial availability of super-bright blue light emitting diodes (LED) and the demonstration of the room temperature blue lasers based on the GaN system are clear indicative of the great potential of this material system.^{2,3} Recently, there has been much work concerning the fundamental optical transitions in GaN.⁴⁻¹² In particular, studies of excitonic transitions in III-nitrides are extremely important for the understating of fundamental properties of these materials as well as for their practical applications. Fundamentally important information regarding exciton binding energy, Bohr radius, exciton-phonon interaction, decay lifetimes, and quantum efficiency can be obtained from these studies.⁵ For practical applications, exciton transitions provides a simple and effective way for calibrating the sample quality. It is well known that excitonic transitions can only be observed in high quality samples and the linewidths of these transitions are directly correlated with parameters such as sample uniformity and stoichiometry. Most importantly, the dynamics of various optical transitions can provide important information regarding excitation and energy transformation processes and recombination lifetimes, which are strongly correlated with quantities such as the quantum efficiency and optical gain in GaN. These basic quantities are crucial for the design of optoelectronic devices. With recent advancement of epitaxial growth techniques, remarkable improvement in crystal quality has been achieved. In order to fully understand fundamental properties as well as to take the full advantages of this new class of materials, the investigations of the fundamental optical transitions and their dynamic processes in these materials become ever increasingly important.

Table I. Structures and parameters of GaN, InGaN epilayers, InGaN/GaN and GaN/AlGaIn MQW samples used in this work.

Growth Method	Sample	Materials	x	Structure	Type	Carrier concentration(cm ⁻³)
MOCVD	A	GaN		Epilayer	n	5 x 10 ¹⁶
	B	GaN		Epilayer	n	2.4 x 10 ¹⁷
	C	GaN		Epilayer	p	1 x 10 ¹⁷
	D	In _x Ga _{1-x} N	0.12	Epilayer	n	
	E	25 Å In _x Ga _{1-x} N/GaN	0.15	MQW		
MBE	G	GaN		Epilayer	Insulating	
	H	25 Å GaN/Al _x Ga _{1-x} N	0.07	MQW		

In this paper, we summarize recent experimental results on the dynamics of fundamental optical transitions in GaN and InGaN epilayers, In_xGa_{1-x}N/GaN and GaN/Al_xGa_{1-x}N multiple quantum wells (MQWs). For GaN epilayers, fundamental optical transitions and their dynamic processes in n- and p-type (Mg doped) and semi-insulating GaN epilayers, including the impurity-bound excitons and free excitons transitions, are summarized. For MQWs, the recombination dynamics of optical transitions in both In_xGa_{1-x}N/GaN and GaN/Al_xGa_{1-x}N MQWs grown by different methods (MOCVD vs. MBE) are compared with each other as well as with GaN and InGaN epilayers. The implications of these results on device applications, in particular on the blue LEDs and laser diodes as well on the lasing mechanisms in GaN blue lasers, are also discussed.

2. EXPERIMENTAL

Samples used in this work include GaN and In_xGa_{1-x}N epilayers and In_xGa_{1-x}N/GaN and GaN/Al_xGa_{1-x}N MQWs grown both by metal-organic chemical vapor depositions (MOCVD) and by reactive molecular beam epitaxy (MBE). Their structures and parameters are summarized in Table I. All samples studied were of wurtzite structure grown on sapphire (Al₂O₃) substrates with AlN buffer layers.

Low temperature time-resolved photoluminescence (PL) spectra were measured by using a picosecond laser spectroscopy system with an average output power of about 20 mW, a tunable photon energy up to 4.5 eV, and a spectral resolution of about 0.2 meV.^{4,5} A micro-channel-plate photomultiplier tube (MCP-PMT) together with a single photon counting system was used to collect time-resolved PL data and the overall time resolution of the detection system was about 20 ps.

3. RESULTS AND DISCUSSIONS

3.1 GaN Epilayers

Figure 1 shows four low-temperature (10 K) PL spectra obtained for samples A, B, C, (MOCVD) and sample G (MBE). For high purity epilayer grown by MOCVD (sample A), two emission lines with energy peak positions at about 3.485 eV and 3.491 eV are identified as due to the recombination of the ground state of free A and B excitons [A(n=1) and B(n=1)] in GaN epilayers.⁹ These assignments are based on the following facts:

- The PL emission intensities, I_{emi} of the 3.485 eV and 3.491 eV lines increase superlinearly with excitation intensity, I_{exc} , following a power-law form, $I_{emi} \propto I_{exc}^\beta$, with $\beta \approx 2$. On the contrary, the donor bound exciton line (I_2) observed in sample B with a higher native donor concentration exhibits a sublinear dependence of I_{emi} on I_{exc} , due to the

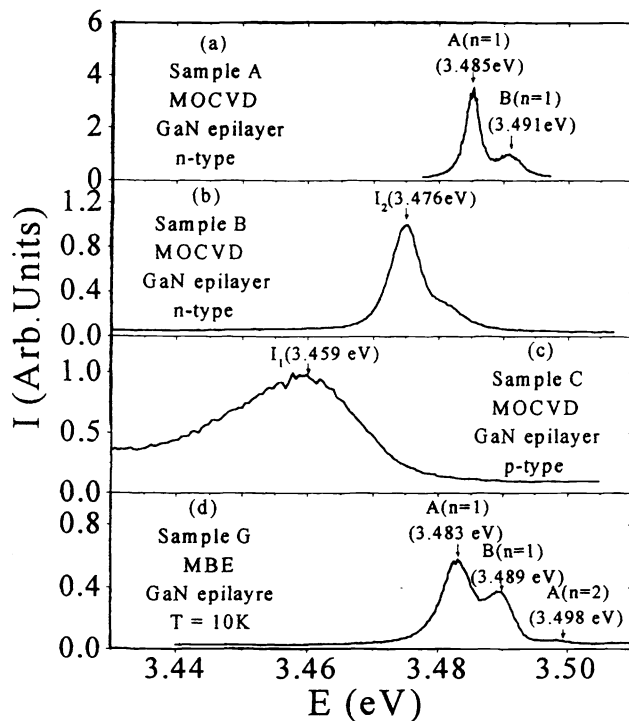


Fig. 1 PL emission spectra of GaN epilayers measured at $T=10$ K.

are comparable.^{5,7,8} An emission line due to the recombination of the first excited state of the A-exciton $A(n=2)$, which is about 14.3 meV above the $A(n=1)$ emission line, is also observable in sample A at $T > 40$ K.⁸ For an as-grown sample with a higher native donor concentration (sample B), the dominant emission line occurs at 3.476 eV and is due to the recombination of the excitons bound to neutral donors, called I_2 .¹⁰ The shoulder at about 3.484 eV in sample B is due to the free A exciton ($n=1$) recombination. Thus the binding energy of the neutral-donor-bound exciton is around 8 or 9 meV. For Mg doped p-type epilayer (sample C), the dominant emission line at 3.459 eV is due to the recombination of neutral-acceptor-bound excitons, called I_1 .¹¹ A value of about 26 meV is thus obtained for the binding energy of the neutral-acceptor-bound exciton in GaN.

In a high quality and purity epilayer grown by MBE (sample G), three emission lines at 3.483 eV, 3.489 eV, and 3.498 eV are observable, which correspond to the transitions of the ground state of A- and B-excitons and the first excited state of the A-exciton ($n=2$), respectively.^{4,7} The energy difference between the first and the ground states of the excitons thus gives the binding energy of the A exciton, $E_b = (4/3) \times (3.498 - 3.483)$ eV = 20 (meV). The energy separation between the A and B valence bands obtained from sample G (6 meV) is consistent with that obtained from sample A. The slight energy difference in the peak positions of the $A(n=1)$ and $B(n=1)$ emission bands observed in MOCVD grown sample (A) and MBE grown sample (G), 3.485 eV vs. 3.483 eV and 3.491 eV vs. 3.489 eV, may be due to a slight difference in strain present in these two different samples. However, among all samples (epilayers grown on sapphire substrates) we have studied, the variation in the A-exciton emission energy position is within 3 meV.

The recombination lifetimes of the optical transitions in GaN including n-type, p-type, and semi-insulating epilayers have been measured.^{4,5,9-12} The temperature dependence of the recombination lifetime of the neutral-donor-bound exciton I_2 transition in sample B measured at its spectral peak positions is shown in Fig. 2(a). The recombination kinetics of the I_2 transition observed at different conditions can be well described by a single exponential function, $I(t) = I_0 e^{-t/\tau}$, where τ defines the recombination lifetimes. The I_2 transition decays very fast with a typical lifetime of about 100 ps at low temperatures.

saturation of impurities;

- (b) The PL emission intensity of the 3.485 eV line decreases with temperature with a thermal activation energy of about 21 meV, which is very close to the A-exciton binding energy (~20 meV) and is much larger than the binding energy of the donor-bound exciton (~8 meV);
- (c) The temperature dependence of the recombination lifetime of the A-exciton and B-excitons are different than that of the bound exciton, which will be discussed later;
- (d) Observation of both the I_2 and the A-exciton transitions at the corresponding energy positions in sample B.

The narrow linewidths of these two emission bands are clear indications of the high crystalline quality of sample A. Our results show that the energy separation between the A and B valence bands is about 6 meV with the assumption that A and B exciton binding energies

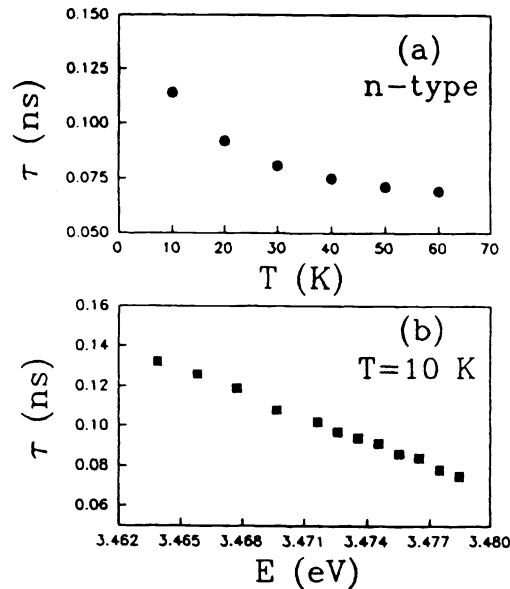


Fig. 2 (a) Temperature dependence of the I_2 recombination lifetime measured at the PL spectral peak positions. (b) Emission energy dependence of the I_2 recombination lifetime measured at $T = 10$ K.

Fig. 2(a) shows that τ decreases with increasing temperature. This behavior is due to the increased nonradiative recombination rate at higher temperatures, related with the dissociation of the neutral-donor-bound excitons, $(D^0, X) \rightarrow D_0 + X$. The radiative recombination lifetime of the I_2 transition can be obtained by extrapolating τ to $T=0$, which is about 130 ps. At temperatures $T > 60$ K, the I_2 recombination lifetimes becomes comparable to the time resolution of our detection system. Fig. 2(b) shows the emission energy dependence of the recombination lifetime of the I_2 transition measured at $T=10$ K, which shows τ decreasing with increasing emission energy. To be discussed below, this emission energy dependence implies the existence of a distribution of the donor-bound exciton binding energy, E_{bx} , in sample B.

We have also measured the emission energy, temperature, and excitation intensity dependencies of the recombination lifetime of the neutral acceptor-bound exciton (I_1) transition line in sample C. The results are presented in Fig.3. Fig. 3(a) shows that at 10 K the recombination lifetime decreases monotonically from 0.56 to 0.30 ns with increasing emission energy, while a large change in τ is observed in the energy region between 3.445 eV and 3.465 eV.

The observed emission energy dependence of the recombination lifetime for both I_1 and I_2 transitions can be explained by a well known theory for bound excitons, which indicates that the radiative recombination lifetime of an impurity bound exciton increases with its binding energy, E_{bx} .¹³ This theory has been confirmed experimentally in many materials. On the other hand, E_{bx} can be written as $E_{bx} = E_g - E_x - hv$, where E_g , E_x , and hv are the energy gap, binding energy of the free-exciton, and emission energy of the bound exciton respectively. Thus, higher emission energies correspond to lower values of E_{bx} . Therefore, the recombination lifetime decreases with an increase of emission energy (hv). The observed behavior suggests the existence of a distribution of E_{bx} due to imperfections in samples B and C.

The temperature dependence of the recombination lifetime of the I_1 transition measured at its spectral peak positions is plotted in Fig. 3(b), which illustrates that τ is independent of temperature below 20 K and decreases with increasing temperature above 20 K. This behavior is again due to the increased recombination rate of the nonradiative processes at higher temperatures, processes such as the bound exciton dissociation to become neutral acceptors and free-excitons, $(A^0, X) \rightarrow A^0 + X$, and subsequent transformation into other recombination channels. The radiative recombination lifetime of the I_1 transition should be close to the value measured at low temperatures and is about 0.45 ns. This value is a little shorter than

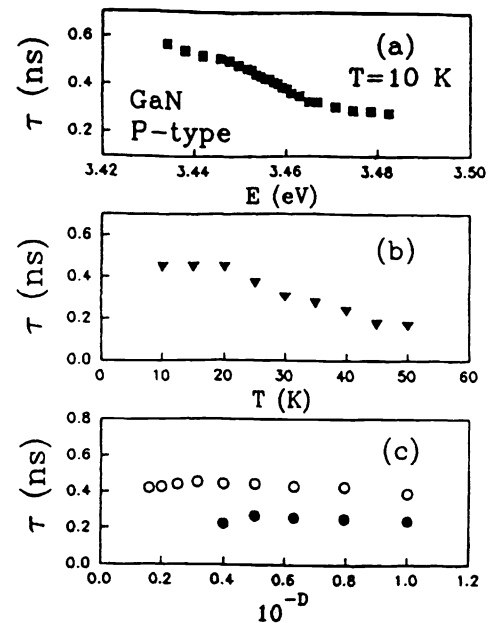


Fig. 3 (a) Emission energy, (b) temperature, and (c) excitation intensity dependencies of the I_1 recombination lifetime measured (a) around the I_1 spectral peak at $T=10$ K, (b) at the I_1 spectral peak positions, and (c) at two representative temperatures $T=10$ (\circ) and 35 K (\bullet).

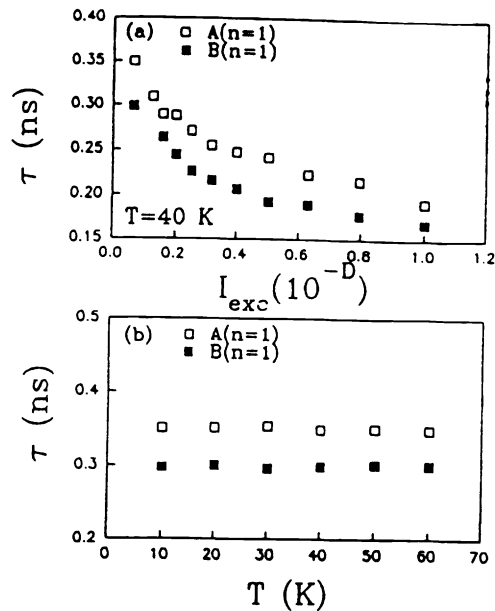


Fig. 4 (a) Excitation intensity $I_{exc} (\propto 10^{-D})$ dependence of the recombination lifetimes of the A(n=1) and B(n=1) excitons measured at their respective spectral peak positions at 40 K. (b) Temperature dependence of the recombination lifetimes of A(n=1) and B(n=1) excitons measured at their respective spectral peak positions and at low excitation intensities.

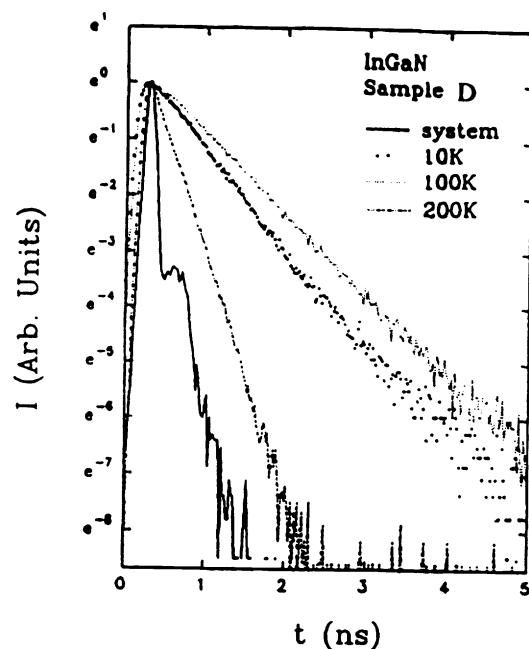


Fig. 5 The PL temporal responses measured at the spectral peak positions for the InGaN epilayer (sample D) at three representative temperatures. The system response to the laser pulses is indicated as "system" and is about 20 ps.

the radiative recombination lifetime of I_1 in well studied CdS materials, which is 0.65 ns.¹⁴ The temperature dependence of the recombination lifetime τ shown in Figs. 2(b) and 3(b) also explains the rapid luminescence intensity quenching of the I_2 and I_1 emission lines at higher temperatures.

The recombination lifetimes of the A- and B-excitons have also been measured in high purity and quality GaN epilayers (sample A and sample G) at low temperatures. The decay of the free exciton luminescence can also be described by a single exponentially, $I(t) = I_0 e^{-t/\tau}$, where τ defines the recombination lifetimes. We have measured the PL temporal responses at different temperatures, emission energies (both A- and B-excitons), and excitation intensities. In all cases, the decay kinetics is a single exponential.

In Fig. 4(a), we have plotted for sample A the recombination lifetimes of the A- and B-excitons measured at their respective emission peak positions at 40 K as functions of relative excitation intensity, $I_{exc} (\propto 10^{-D})$. The B-exciton recombination lifetimes are about 15% shorter than those of the A-excitons. The lifetime drops from 0.35 ns to 0.20 ns for the A-exciton, while it decreases from 0.3 to 0.17 ns for the B-exciton as the relative excitation intensity is increased from 0.1 to 1.0. We attribute the observed behavior to exciton-exciton interaction, which causes a reduction in the free-exciton recombination lifetime. However, such an interaction is absent at low free-exciton densities. By extrapolating the lifetime to the lowest excitation intensity, one obtains recombination lifetimes to be about 0.35 ns for the A-excitons and 0.3 ns for the B-excitons.

The temperature dependence ($T < 60$ K) of the recombination lifetime of A(n=1) and B(n=1) measured at low excitation intensity is shown in Fig. 4(b). The lifetimes of both A- and B-excitons are independent of temperature below 60 K, which may imply that the radiative recombination is the dominant process at $T < 60$ K, otherwise a strong temperature dependence, such as the temperature dependence of the I_2 and I_1 recombination lifetimes (Figs. 2(a) and 3(b)), is expected. Additionally, from the temperature independent behavior of the recombination lifetimes, we expect that their excitation intensity dependencies at different temperatures are the same as those shown in Fig. 4(a). Thus the radiative recombination lifetimes of single exciton can be obtained by extrapolating the curves in Fig. 4 to the lowest excitation intensity. The results thus suggest that (a) the radiative recombination lifetimes for single exciton are about 0.35 and 0.3 ns for the A- and B-excitons,

Table II. Fundamental optical transitions in GaN epilayers grown on sapphire substrates.

Transition Lines	Positions		Width (meV)	Lifetime (ns)
	(Å)	(eV)		
I ₁	3584.4	3.459	23	0.45
I ₂	3566.9	3.476	4.6	0.12
A(n=1)	3557.7	3.485	1.7	0.35
B(n=1)	3551.4	3.491	4.0	0.30
A(n=2)	3543.4	3.499	8.0	not available

respectively and (b) the radiative decay rate increases with an increase of excitation power for both A- and B-excitons, which has resulted in an enhanced PL quantum yield.

We have summarized the results of GaN epilayers in Table II, where the emission peak positions, full width at half maxima (FWHM) and the recombination lifetimes of I₁, I₂, the ground states of A and B excitons, A(n=1) and B(n=1), and the first excited state of A-exciton, A(n=2), measured at low temperatures are listed. The ratio of the recombination lifetime of I₁ to I₂, $\tau(I_1)/\tau(I_2) = (0.45 \text{ ns}/0.12 \text{ ns})$, is in a reasonable agreement with the ratio of the binding energy of I₁ to I₂, $E_{bx}(I_1)/E_{bx}(I_2) = 26 \text{ meV}/8 \text{ meV}$.

3.2 InGaN Epilayers

PL emission spectrum of a MOCVD grown InGaN epilayer (sample D) measured at 10 K is red shifted with respect to that of GaN epilayers due to In incorporation. Another effect is that the emission linewidth of the InGaN epilayer is more than one order of magnitude larger than those of GaN epilayers due to alloy disorder. To be shown in Fig. 6(a), the emission peak position in sample D is at about 3.193 eV with a full linewidth at half maximum (FWHM) of about 55 meV, which is due to the recombination of localized excitons. In an alloy, the exciton localization is caused by energy fluctuations in the band edge induced by alloy disorder and the linewidth is correlated with the exciton localization energy.

The recombination dynamics of the PL emissions in the In_xGa_{1-x}N epilayer (sample D) have been measured. Fig. 5 shows the temporal responses of the localized exciton recombination resulting from sample D measured at the spectral peak positions at three different temperatures T=10, 100, and 200 K. The detection system response to the laser pulses is also indicated as "system", which is about 20 ps. As shown in Fig. 5, the PL decay in In_xGa_{1-x}N epilayers can be described quite well by a single exponential at all temperatures. The PL recombination lifetimes, τ , were measured at the spectral peak positions from 10 K to room temperature.¹⁵ At room temperature, the values of τ is about 0.1 ns. To be shown in Fig. 7(b), the localized exciton lifetime in the In_xGa_{1-x}N epilayer is about 0.53 ns at T < 40 K and then **increases** almost linearly with temperature up to 100 K. The longest radiative decay lifetime seen in In_xGa_{1-x}N epilayer is 0.70 ns at 100 K.

The low temperature PL recombination lifetime in In_xGa_{1-x}N is also a function of emission energy and excitation intensity (not shown). Such an emission energy dependence of τ is a characteristic of localized excitons in semiconductor alloys.¹⁶ On the other hand, the radiative recombination lifetimes of localized excitons in In_xGa_{1-x}N sample decrease with an increase of excitation intensity, similar to the behavior of the free-excitons in GaN.⁹⁻¹¹

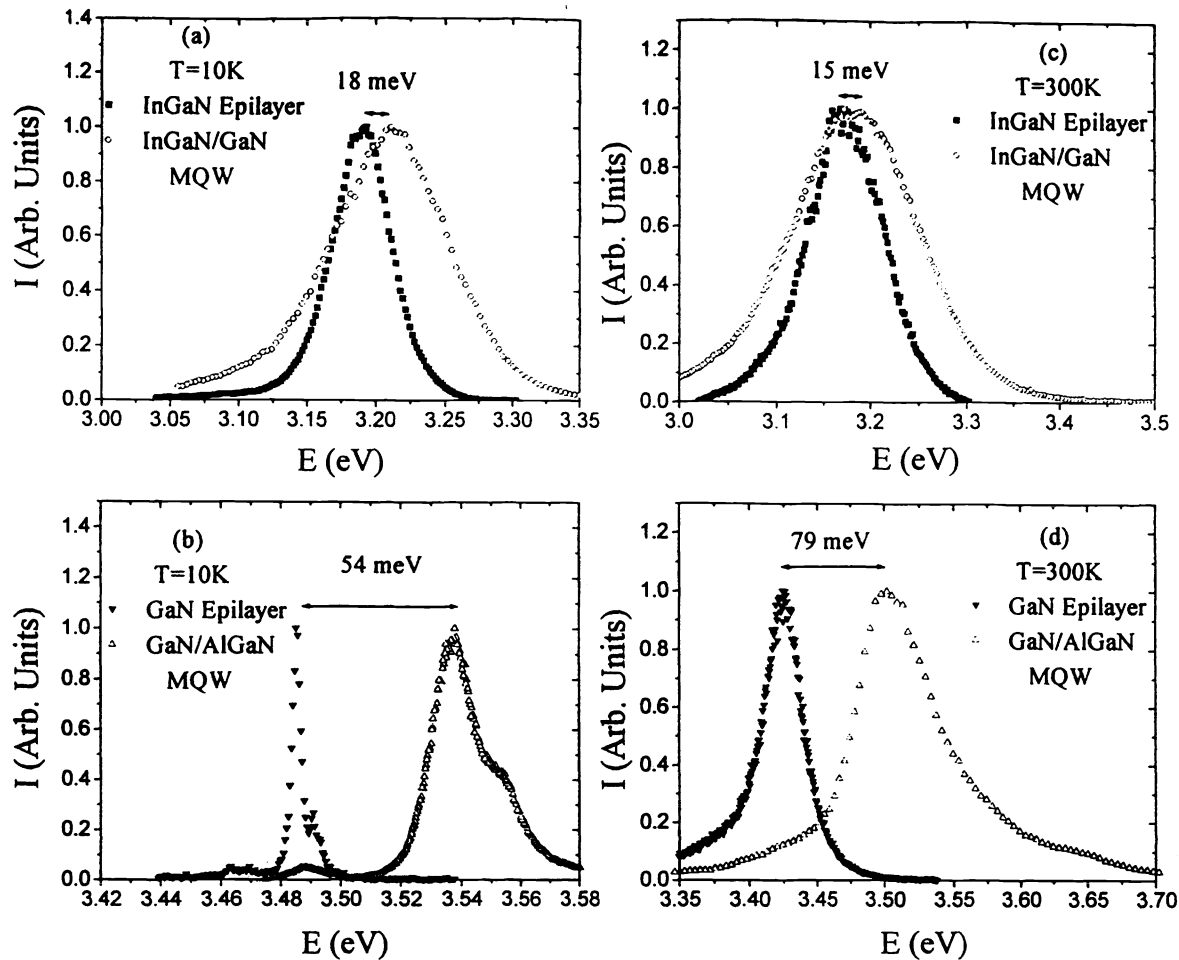


FIG. 6. CW PL spectra of an InGaN epilayer (filled squares) and $\text{In}_x\text{Ga}_{1-x}\text{N}/\text{GaN}$ MQW (open circles) measured at (a) $T=10\text{ K}$ and (c) $T=300\text{ K}$, and of a GaN epilayer (filled triangles) and $\text{GaN}/\text{Al}_x\text{Ga}_{1-x}\text{N}$ MQW (open triangles) measured at (b) $T=10\text{ K}$ and (d) $T=300\text{ K}$.

3.3 *InGaN/GaN and GaN/AlGaN MQWs*

In Fig. 6, we plotted the CW PL spectra of a MOCVD grown $\text{In}_x\text{Ga}_{1-x}\text{N}/\text{GaN}$ MQW sample (sample E) obtained at (a) $T=10\text{ K}$ and (c) $T=300\text{ K}$ (open circles). For comparison, the PL spectra of the MOCVD grown InGaN epilayer (sample D) are also shown. We have also plotted the CW PL spectra of the MBE grown $\text{GaN}/\text{Al}_x\text{Ga}_{1-x}\text{N}$ MQW sample (sample H) obtained at (b) $T=10\text{ K}$ and (d) $T=300\text{ K}$ (open triangles). The PL spectra of the MBE grown GaN epilayer (sample G) are also shown for comparison. In the $\text{In}_x\text{Ga}_{1-x}\text{N}$ epilayer, the dominant transition line at low temperature is from the recombination of localized excitons. As can be seen, the transition peak position in the $\text{In}_x\text{Ga}_{1-x}\text{N}/\text{GaN}$ MQW is blue shifted. The amount of blue shift is about $18 \pm 2\text{ meV}$. Fig. 6(b) and (d) also clearly show the blue shift of the transitions in $\text{GaN}/\text{Al}_x\text{Ga}_{1-x}\text{N}$ MQW respect to the GaN epilayers. The blue shift of the emission line from the GaN/AlGaN MQW at room temperature (79 meV) is what we expected for our MQW structure with a 67% (33%) conduction (valence) band offset. One of the interesting features shown in Fig. 6 is that the blue shift observed at 10 K is only 54 meV for the $\text{GaN}/\text{Al}_x\text{Ga}_{1-x}\text{N}$ MQW structure, or about 25 meV less than the shift at room temperature. We attribute this difference to the fact that the PL emissions in the $\text{GaN}/\text{Al}_x\text{Ga}_{1-x}\text{N}$ MQW at low and room temperatures result from the recombination of localized and free excitons, respectively. The exciton localization at low temperatures is caused by interface roughness of the MQW. The 25 meV difference then measures the localization energy, indicating a well thickness fluctuation of about $\pm 4\text{ \AA}$.

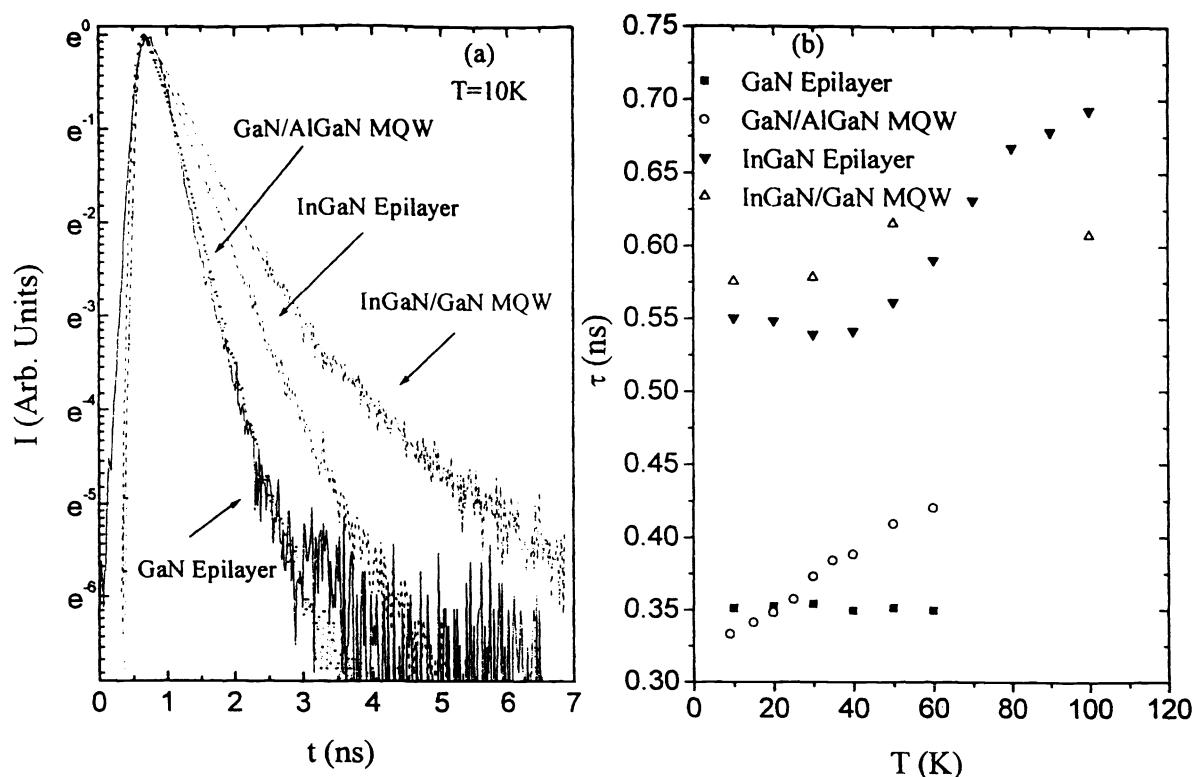


FIG. 7. (a) The temporal responses of the PL measured at the spectral peak positions in GaN and InGaIn epilayers, and InGaIn/GaN and AlGaIn/GaN MQW at $T=10\text{K}$. (b) Temperature dependence of the recombination lifetimes at low temperatures.

The recombination dynamics of the PL emission in $\text{In}_x\text{Ga}_{1-x}\text{N}/\text{GaN}$ and $\text{GaN}/\text{Al}_x\text{Ga}_{1-x}\text{N}$ MQWs have also been measured. Fig. 7(a) shows the temporal responses of PL resulting from the GaN epilayer, $\text{GaN}/\text{Al}_x\text{Ga}_{1-x}\text{N}$ MQW, $\text{In}_x\text{Ga}_{1-x}\text{N}$ epilayer, and the $\text{In}_x\text{Ga}_{1-x}\text{N}/\text{GaN}$ MQW measured at the PL spectral peak positions at $T=10\text{K}$. PL decay in all samples, except the $\text{In}_x\text{Ga}_{1-x}\text{N}/\text{GaN}$ MQW, can be well described by a single exponential decay. The PL decay in the $\text{In}_x\text{Ga}_{1-x}\text{N}/\text{GaN}$ MQW was fit using a two-exponential function with the fast component contributing over 85% of the PL signal. The temperature dependencies of the recombination lifetime τ are shown in Fig. 7(b). In the $\text{In}_x\text{Ga}_{1-x}\text{N}$ epilayer (filled triangle), the localized exciton lifetime is about 0.53 ns at $T < 40\text{K}$ and increases almost linearly with temperature from 40 K up to 100 K. Comparing this with the $\text{In}_x\text{Ga}_{1-x}\text{N}/\text{GaN}$ MQW (open triangle), where only the recombination lifetime of the fast component is plotted, only a slight temperature dependency of the recombination lifetime is seen up to 100 K. Consider the GaN epilayer (filled square), the recombination lifetime of the A-exciton ($\sim 0.35\text{ns}$) is nearly temperature independent below 60 K. In the $\text{GaN}/\text{Al}_x\text{Ga}_{1-x}\text{N}$ MQW (open circle), however, τ increases linearly with temperature up to 60 K.

As illustrated clearly in Fig. 7 (b), all high quality samples seem to have recombination lifetimes which are either temperature independent, or increase linearly with increasing temperature at low temperatures. A similar linear behavior at low temperatures has been observed previously in $\text{GaAs}/\text{Al}_x\text{Ga}_{1-x}\text{As}$ MQW samples and is now regarded as a unique property of radiative excitonic recombination.¹⁶ Thus, we see that radiative recombination is the dominant process in all samples at low temperatures. A summary of these results can be seen in Table III, which also includes results from $\text{GaAs}/\text{Al}_x\text{Ga}_{1-x}\text{As}$ MQW for comparison. Comparing the behavior between the three MQW of comparable well size, the behavior of the $\text{In}_x\text{Ga}_{1-x}\text{N}/\text{GaN}$ MQW stands out. It shows no clear linear dependence, unlike the $\text{GaN}/\text{Al}_x\text{Ga}_{1-x}\text{N}$ MQW and the $\text{GaAs}/\text{Al}_x\text{Ga}_{1-x}\text{As}$ MQW.¹⁷ The slope of τ vs temperature T , $d\tau/dT$, for the $\text{GaN}/\text{Al}_x\text{Ga}_{1-x}\text{N}$ MQW is about $1.8 \times 10^{-3}\text{ns/K}$ while that of the $\text{GaAs}/\text{AlGaAs}$

TABLE III. Recombination lifetime behavior of epilayers and MQW

Well (Å)	MOCVD	MOCVD	MOCVD	MBE ³	MBE	MBE ⁵		
	InGa _x N/GaN MQW	InGa _x N Epilayer	GaN Epilayer	GaN Epilayer	GaN/AlGa _x N MQW	GaAs/AlGaAs MQW		
Temperature (K)	25	—	—	—	25	25	40	55
$d\tau/dT$ (10^{-3} ns/K)	100	$40 \leq T \leq 100$	≤ 60	≤ 30	≤ 60	≤ 30	≤ 25	≤ 20
τ_0 (ns)	—	4	~ 0	~ 0	1.8	17.5	58.8	33.8
	0.57	0.54	0.35	0.22	0.32	0.32	0.44	0.82

of the same well with is about 1.7×10^{-2} ns/K. The high quality In_xGa_{1-x}N epilayer, on the other hand, does show this linear dependence, with a slope $d\tau/dT \sim 4 \times 10^{-3}$ ns/K, unlike the GaN epilayer samples which have a constant recombination lifetime at low temperatures. By extrapolating the plots in Fig. 7(b) to $T=0$ K, the radiative recombination lifetime τ_0 , of the samples can be determined.

3.4 Origin of Room Temperature Intrinsic Transitions in GaN

We have also investigated the mechanism of room temperature intrinsic transition in high quality MOCVD grown GaN epilayers (e.g., sample A).¹⁸ Fig. 8(a) shows the room temperature PL emission spectra of sample A measured at different excitation intensities, I_{exc} . We see that the intrinsic transition spectral peak position, E_p , shifts toward the lower emission energies. More importantly, as illustrated in Fig. 8(b) the red shift with I_{exc} follows exactly the expression, $\Delta E_p \sim I_{exc}^{1/3}$. This is a consequence of the free carrier screening effect¹⁹ and gives the direct evidence for the band-to-band transition in GaN epilayers at room temperature. The observation of the band-to-band transition at room temperature is partly due to the presence of relatively high native donor concentrations in MOCVD grown GaN epilayers. Presently, the native donor concentration in best GaN epilayers is around 5×10^{16} cm⁻³.

The observation of the band-to-band transition at room temperature in GaN raises an interesting issue, as this transition is rarely observable in high quality and purity II-VI and other III-V semiconductors. A particular example is the GaAs/AlGaAs system in which the binding energy of the excitons is only a few meV, but the exciton transition is still the dominant transition even at room temperature. This is due to the much smaller radiative recombination rate (or much longer radiative recombination lifetime) of the band-to-band transition than that of the exciton transition in the GaAs system. In the GaN materials, our results indicate that the recombination rates of these two intrinsic transitions may be of the same order. One immediate consequence of these results is that the electron-hole plasma would most likely be responsible for gain in GaN lasers because the band-to-band transition is the most dominant optical transition in high quality GaN epilayers at room temperature.

4. SUMMARY

In summary, recent experimental results on the dynamics of fundamental optical transitions in GaN and InGa_xN epilayers, In_xGa_{1-x}N/GaN and GaN/Al_xGa_{1-x}N multiple quantum wells (MQWs), probed by picosecond time-resolved PL emission spectroscopy, have been summarized. For GaN epilayers, optical transitions in n- and p-type (Mg doped) and semi-insulating GaN epilayers have been studied. Recombination lifetimes of fundamental optical transitions, including the impurity-bound excitons and free excitons transitions, have been discussed. For MQWs, recombination dynamics of optical transitions in both In_xGa_{1-x}N/GaN and GaN/Al_xGa_{1-x}N MQWs grown by different methods (MOCVD vs. MBE) have been compared with each other as well as with GaN and InGa_xN epilayers. The implications of these results on device applications, in particular on the blue LEDs and laser diodes have also been discussed.

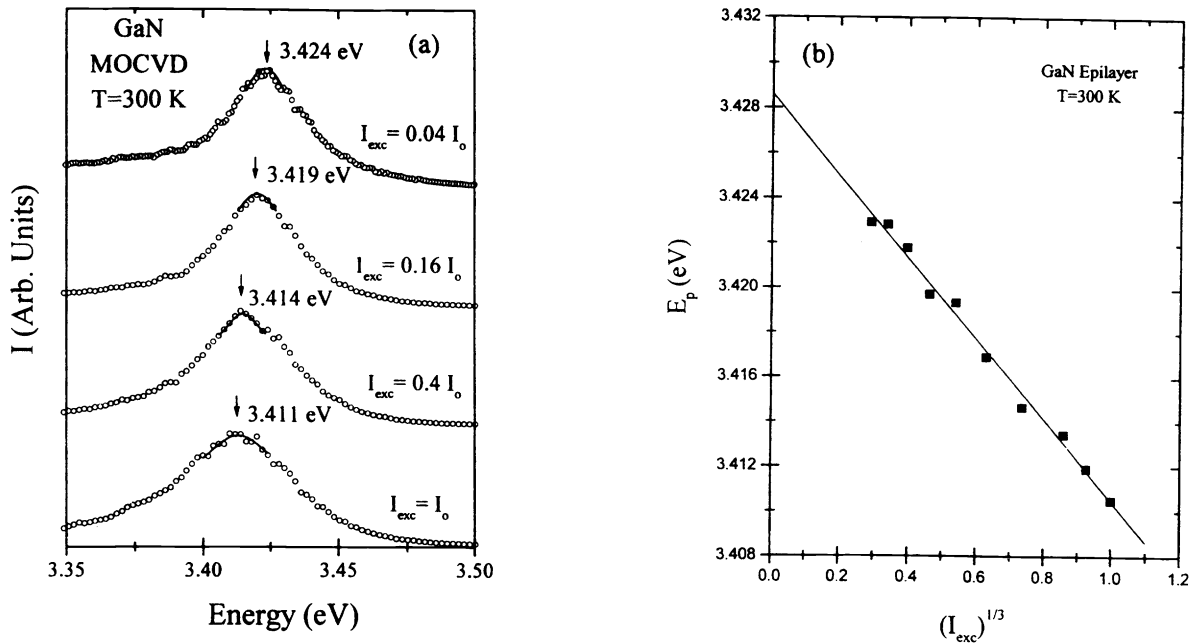


Fig. 8 (a) cw PL spectra of sample A measured at $T = 300$ K for several representative I_{exc} . The solid lines near the PL maxima are the least-squares fit of data using the Gaussian functions and the arrows indicate the fitted peak positions. (b) The spectral peak positions of the PL emission line in samples A measured at 300 K, E_p vs $(I_{exc})^{1/3}$. The solid line is the least-squares fit of data with a linear equation, $E_p \propto (I_{exc})^{1/3}$.

5. ACKNOWLEDGMENTS

The work is supported by ARO and BMDO (monitored by Dr. John Zavada, Dr. Yoon S. Park of ONR, and Dr. K. P. Wu), DOE (96ER45604/A000), and NSF (DMR-9528226). We are grateful to Professors H. Morkoc and Asif Khan for their long-time collaboration and support. We also acknowledge assistance from former and present group members in our group, M. Smith, K. C. Zeng, R. Mair, J. Z. Li, C. Ellis, and G. D. Chen.

6. REFERENCES

1. H. Morkoc, S. Strite, G. B. Gao, M. E. Lin, B. Sverdlov, and M. Burns, *J. Appl. Phys.* **76**, 1363 (1993); S. N. Mohammad, A. Salvador, and H. Morkoc, *Proc. IEEE*, **83**, 1306 (1995).
2. S. Nakamura, M. Senoh, N. Iwasa, and S. Nagahama, *Jpn. J. Appl. Phys.* **34**, L797 (1995).
3. S. Nakamura, M. Senoh, N. Iwasa, S. Nagahama, N. Iwasa, T. Yamada, T. Matsushita, H. Kiyoku, and Y. Sugimoto, *Appl. Phys. Lett.* **68**, 2105(1996).
4. M. Smith, G. D. Chen, J. Z. Li, J. Y. Lin, H. X. Jiang, A. Salvador, W. K. Kim, O. Aktas, A. Botchkarev, and H. Morkoc, *Appl. Phys. Lett.* **67**, 3387 (1995).
5. G. D. Chen, M. Smith, J. Y. Lin, H. X. Jiang, S. H. Wei, M. Asif Khan, and C. J. Sun, *Appl. Phys. Lett.* **68**, 2784 (1996).
6. C. I. Harris, B. Monemar, H. Amano, and I. Akasaki, *Appl. Phys. Lett.* **67**, 840 (1995).
7. D. C. Reynolds, D. C. Look, W. Kim, Ö. Aktas, A. Botchkarev, A. Salvador, H. Morkoc, and D. N. Talwar, *J. Appl. Phys.*, **80**, 594 (1996).

8. W. Shan, B. D. Little, A. J. Fischer, J. J. Song, B. Goldenberg, W. G. Perry, M. D. Bremser, and R. F. Davis, *Phys. Rev.* **B54**, 16369 (1996).
9. M. Smith, G. D. Chen, J. Y. Lin, H. X. Jiang, M. Asif Khan, C. J. Sun, Q. Chen, and J. W. Yang, *J. Appl. Phys.* **79**, 7001 (1996).
10. G. D. Chen, M. Smith, J. Y. Lin, H. X. Jiang, M. Asif Khan, and C. J. Sun, *Appl. Phys. Lett.* **67**, 1653 (1995).
11. M. Smith, G. D. Chen, J. Y. Lin, H. X. Jiang, M. Asif Khan, and C. J. Sun, *Appl. Phys. Lett.* **67**, 3295 (1995).
12. M. Smith, J. Y. Lin, H. X. Jiang, A. Salvador, A. Botchkarev, W. K. Kim, and H. Morkoc, *Appl. Phys. Lett.* **69**, 2453 (1996).
13. E. L. Rashba and G. E. Gurgenishvili, *Sov. Phys. Solid State* **4**, 759 (1962).
14. R. Heitz, C. Frickel, A. Hoffmann, and I. Broser, *Mater. Sci. Forum* **83-87**, 1241 (1992).
15. M. Smith, G. D. Chen, J. Y. Lin, H. X. Jiang, M. Asif Khan, and Q. Chen, *Appl. Phys. Lett.* **69**, 2837 (1996).
16. H. X. Jiang, L. Q. Zu, and J. Y. Lin, *Phys. Rev.* **B42**, 7284 (1990).
17. J. Feldmann, G. Peter, E. O. Gobel, P. Dawson, K. Moore, C. Foxon, and R. J. Elliott, *Phys. Rev. Lett.* **59**, 2337 (1987).
18. M. Smith, J. Y. Lin, H. X. Jiang, and M. Asif Khan, *Appl. Phys. Lett.* **71**, 635 (1997).
19. R. A. Abram, G. J. Rees, and B. L. H. Wilson, *Adv. Phys.* **27**, 799 (1978).